PRELIMINARY APPLICATION OF SIMPLIFIED FRAGILITY MODELLING ON BUDGET ALLOCATIONS FOR BUILDING PORTFOLIO SEISMIC RETROFIT

A. Cimmino[1], R. Gentile[2], F. Ceroni[1] & N. Caterino[1,3]

[1] University of Naples "Parthenope" - Engineering Department, Italy, Naples, Italy,
antonio.cimmino@studenti.uniparthenope.it

[2] University College London - Institute for Risk and Disaster Reduction, London, UK

[3] Institute of Technologies for Construction - National Research Council of Italy, Milan, Italy

Abstract: *Seismic risk reduction plays a key role in the achievement of a more resilient society, especially for densely populated cities in moderate-to-high seismicity areas characterised by a high vulnerability of the built environment. Since limited resources are usually allocated for risk reduction measures (e.g., building retrofit), defining a risk prioritization scheme to rationally distribute the budget is fundamental. Risk assessment of large building portfolios including several building classes often requires simplified fragility estimation methods. This paper aims to implement a budget allocation framework for building portfolios by adopting a simplified fragility estimation method. This is exemplified by considering an ideal-but-realistic portfolio of buildings representing Italian reinforced concrete schools. The fragility of each relevant building class in the portfolio is evaluated using Simple Lateral Mechanism Analysis (SLaMA). For each class, potential retrofit solutions with increasing levels of building performance are considered. The optimal combination of retrofit interventions is defined as the one that minimizes the portfolio seismic risk constrained to a limited budget. The solution is obtained using an optimization algorithm, effectively balancing accuracy while mitigating computational demands.*

1   Introduction

Several countries, including Italy, Greece, and Turkey are characterized by the presence of large cities located in moderate-to-high seismicity regions and involving a highly vulnerable built environment (often not complying with adequate seismic-resistant criteria). The combination of these key factors highlights the risk of casualties and economic losses when a significant earthquake occurs as evidenced by past seismic events (e.g., Masi et al. (2019)). In the field of seismic risk management, portfolio seismic risk assessments represent a fundamental process to comprehensively evaluate the potential impact of seismic events on a collection of buildings or infrastructures. This process involves a detailed analysis of seismic hazards, building exposure, fragility, and potential losses. Seismic risk reduction measures include a range of strategies and actions designed to minimize the impact of earthquakes on people, buildings, and infrastructure. Commonly, seismic risk mitigation measures encompass structural retrofitting techniques, which are aimed at reducing the vulnerability of existing buildings by improving their performance when subjected to ground shaking. A wide range of structural retrofitting techniques are available, and the choice of the most suitable one depends on several factors like building vulnerability, occupancy, budget available, and local design codes. Selecting the right strategy is crucial for enhancing safety and performance in both the short and long term. In portfolio seismic risk management, a critical challenge is determining the level of retrofitting to be applied conveniently

to each building in a portfolio when limited budget are available. This allows distributing economic resources to maximize the benefits expressed as overall seismic risk reduction. This topic has been already investigated in the literature (Yoshikawa and Goda (2014), Rincòn et al. (2017), Caterino et al. (2018). For example, Caterino et al. (2018) proposed a risk-based decision-making process applied to an ideal portfolio of reinforced concrete school buildings, evaluating overall risk through fragility analysis and a simplified pushover method. This study adopts a similar concept with three main differences, involving: 1) a different simplified mechanics-based fragility estimation method, which takes into account all mechanisms at beam-column joint level; 2) a fragility-based retrofit design procedure to define possible retrofit solutions for each building; 3) an optimization method to allocate resources.

Each building in the portfolio is assigned to a building class, and a seismic fragility analysis is conducted for each class. The use of simplified pushover-based fragility analysis methods provides an acceptable compromise between accuracy and computational effort (Gentile and Galasso, (2021a)). Nevertheless, several simplified methods and procedures have been developed in the last decades (e.g., Calvi (1999), Borzi et al. (2008), Del Gaudio et al. (2015), Gentile et al. (2019)) in this study, attention is focussed on the Simple Lateral Mechanism Analysis (SLaMA, Gentile et al. (2019), NZSEE (2017)). SLaMA is an analytical method that, combined with the Capacity Spectrum Method (CSM, Freeman (1998)), allows calculating the nonlinear force-displacement capacity curve and the plastic mechanism of a building. It's worth noting that the SLaMA procedure adopted herein is fully compliant, with the New Zealand building code (NZSEE (2017)). This code allows the use of different stress-strain models for concrete and steel, along with the adoption of specific drift limits associated with the activation of the beam-column-joint (BCJ) mechanism. This assumption may result in a higher ductility estimate for structural elements compared to the Italian building code standard.

To optimize the risk reduction and achieve a more efficient budget allocation, multiple seismic retrofit configurations with increased performance should be considered. However, performing a fragility assessment of each level of retrofitting can be prohibitively expensive, especially when the number of buildings classes is high. To overcome this issue, a pragmatic approach focused on fragility proposed by Aljawhari et al. (2022) is applied in this paper. Specifically, the increase of displacement-based capacity-on-demand ratio (CDR) at the life-safety (LS) limit state, CDR_{LS}, due to retrofitting is correlated with the corresponding shift in the fragility median values of multiple structure-specific damage states and a pseudo-linear trend can be assumed under certain conditions. In particular, the CDR_{LS} is defined as the ratio of the displacement capacity to demand at the life-safety condition estimated with a pushover based method (e.g. Capacity Spectrum Method).

Finally, the Mixed Integer Linear Programming (MILP) optimization method (Westerberg et al. (1977)) is used to allocate building resources. MILP provides an efficient and systematic approach, allowing us to navigate the complex solution space and identify an optimal solution with reduced computational effort.

By applying the methodology to an ideal portfolio of school buildings, this work aims at providing preliminary insights on the effect of using a simplified fragility estimation method on the optimal solution for resource allocation. The goal is to identify a combination of such interventions that minimizes the seismic risk of the portfolio. To this aim, it is necessary to estimate the seismic risk of all buildings in both the as built and retrofitted configurations, by means of an appropriate loss metric, that, in this study, is assumed as the Expected Annual Loss (EAL). Section 2 provides an overview of the methodology adopted with a brief description of each step. An application of the procedure is described in section 3 with reference to an ideal portfolio of buildings located close to L'Aquila (Italy). Conclusions are provided in section 4.

2   Methodology

The main steps of the adopted procedure (Figure 1) are:

1. Adopt a set of building classes that are representative of the analysed building portfolio. Building classes can be identified using an exposure taxonomy, for example based on geometric parameters (number of stories, span length, etc.), type of lateral load resisting system (frame, wall, dual system, etc.), age of construction (which can be associated with the level of seismic design), etc.;

2. Building classes are analysed using Simple Lateral Mechanism Analysis (SLaMA, Gentile et al. (2019), NZSEE (2017)) to study their force-displacement behaviour under horizontal actions as well as the collapse mechanism;

3. For each building class, one or two retrofit template configurations are provided. The retrofit templates should be designed to improve the seismic behaviour of the building class and prevent any fragile mechanism in the structural members;

4. Perform the seismic response analysis of each building class (as built and retrofitted) with a pushover-based method (e.g. Capacity Spectrum Method, N2 method, etc…) by using code conforming design spectra at Life-Safety (LS) limit state and derive the displacement-based capacity-on-demand ratio at LS limit state (CDR_{LS}) for each configuration.

5. Perform a fragility analysis of each building class (for both the as built and retrofitted configurations of the buildings) with the above pushover method and a set of natural ground motion spectra. In this study, the fragility assessment is consistent with the cloud-analysis method (Jalayer and Cornell (2009)) and it is performed with the Cloud Capacity Spectrum Method (Nettis et al. 2021);

6. For each building class, plot the increase in CDR_{LS}, resulting from retrofitting, to the median of the fragility relationships. This will allow having a proxy of the fragility median for retrofit configurations targeted to reach a specific value of the CDR_{LS} only (i.e., without running further response analyses);

7. Perform a vulnerability analysis of each building class (in as built and all retrofit configurations), assuming a consequence model for each considered damage state (DS);

8. For each building in the portfolio, the Expected Annual Loss (EAL) is calculated for all retrofit configurations adopting the defined vulnerability curves and assuming a site-specific hazard curve. The cost of each retrofit intervention is provided by a literature cost model;

9. The portfolio seismic risk is obtained by summing up the EAL for each building according to its specific vulnerability and hazard. The possible solutions will foresee a different intervention for each building and consequently a different budget allocation. The best solution is the one where the total expected annual loss (EAL_{tot}) is minimized while the investment cost complies with the available budget. The best combination of structural retrofitting interventions is detected applying Mixed-Integer Linear Programming (MILP) optimization method.
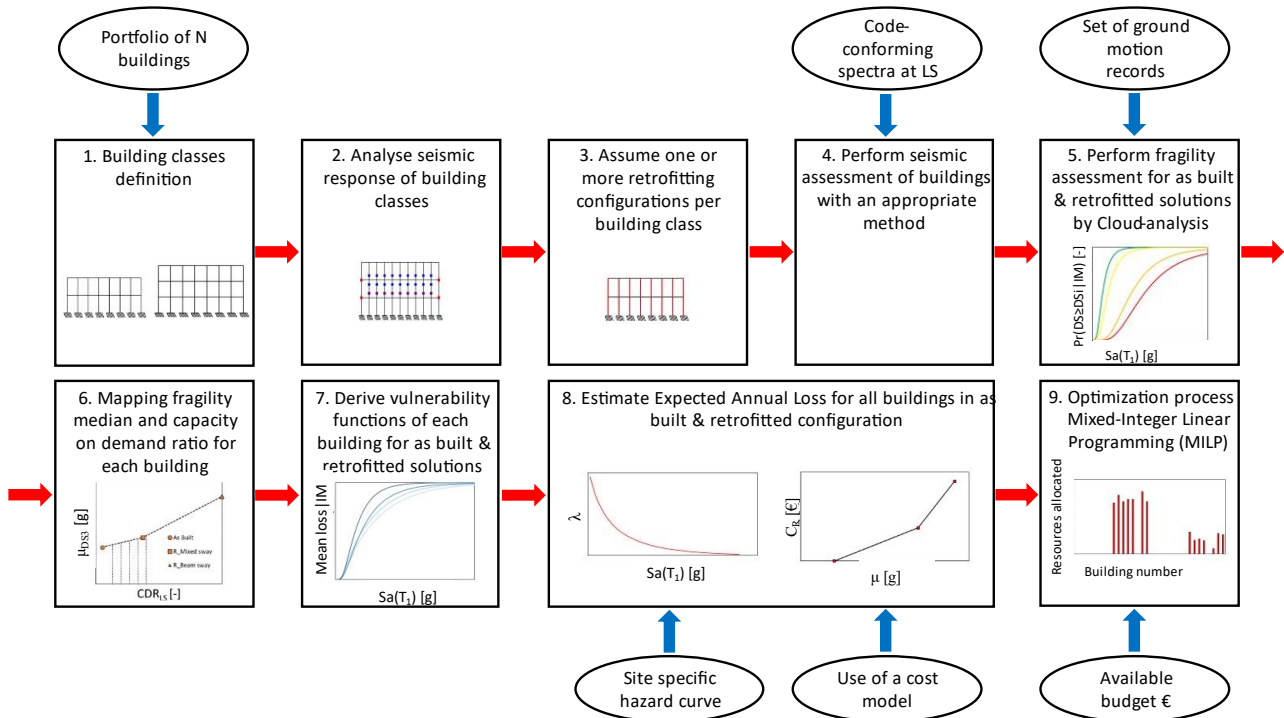

Figure 1. Main steps of the adopted procedure.

3   Case study application

3.1   Building portfolio

An ideal portfolio of 32 school buildings located in municipalities close to L'Aquila (Italy) is investigated (Figure 2a). For each site, the seismic hazard curve is defined starting from the spectral parameters provided by the Italian Building Code "NTC2018". Given N buildings in a portfolio, the first step is to define a limited group of building classes representatives of the buildings. In this work, four building classes representative of Italian gravity load-designed reinforced concrete school buildings are considered (Figure 2b). Each building in the portfolio is assigned to one of the building classes considered in this study.

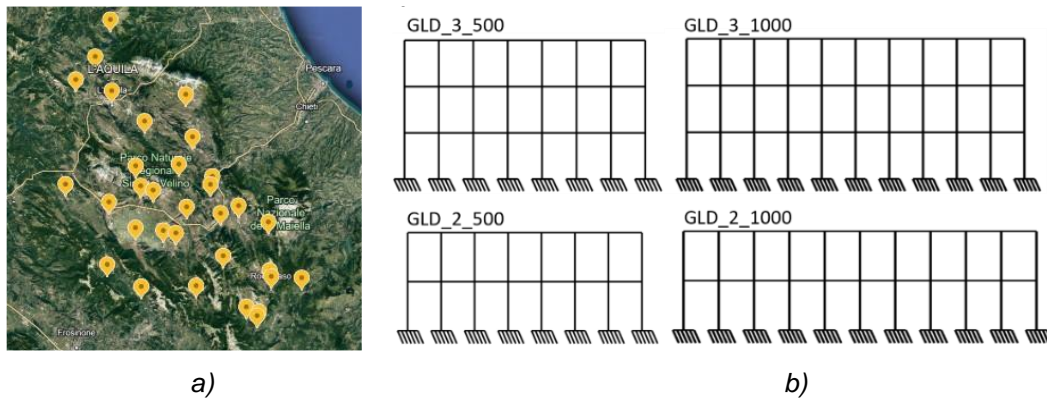| a) | b) |

Figure 2. a) Ideal portfolio with buildings in the municipalities close to L'Aquila (Italy); b) Gravity Load Design (GLD) building classes depending on number of floors (2 or 3) and surface (500 or 1000 m^2).

3.2   As-built seismic assessment

The non-linear capacity of the as-built building configuration for each class is assessed with SLaMA (Gentile et al. (2019)). The first step of SLaMA is to characterise the lateral response of the main structural elements (beams, columns, and beam-column joints) within the frame. The interaction between these elements in the beam-column joint is analysed using the hierarchy of strength principle. Once the failure mode of the sub-assembly has been identified, its strength and deformation capacity are evaluated using equilibrium principles. The results in terms of hierarchy of strength indicate the probable plastic mechanism of the frame. Equations are provided to calculate the capacity curve for three common plastic mechanisms:

1.   "Column-Sway" (soft-story): plastic hinges at the top and bottom of all columns on a given story.

2.   "Beam-Sway": a global mechanism with plastic hinges at the ends of all beams.

3.   "Mixed-Sway": a combination of beam, column, and/or joint failures can be triggered.

The SLaMA pushover curve allows the definition of thresholds for structural and non-structural DS for each building class. Four DS are considered in line with Limit States provided in the Italian Building Code (DS1 - Stato Limite di Operatività, DS2 - Stato Limite di Danno, DS3 - Stato Limite di Salvaguardia della Vita, DS4 - Stato Limite di Collasso). In addition, the damage state DS0, which corresponds to the case of no damage, is added for vulnerability assessment. Each DS occurs when the structure attains a specific threshold defined with respect to an Engineering Demand Parameter (EDP) which is here assumed as the displacement at effective height (H_{eff}). In particular, DS3 and DS4 are defined by the displacement at which the 75% and 100% of ultimate deformation capacity is reached by the first structural element, respectively; moreover, DS1 and DS2, often considered as proxies for non-structural damage, are defined by the displacement corresponding to the attainment of 67% and 100% of the yielding deformation capacity of the first element, respectively.

Figure 3 shows the application of as-built pushover curves for the GLD-3-500 building class derived with SLaMA and the thresholds related to different DSs. The results are consistent across the four building classes: shear mechanisms at the beam-column joint (BCJ) nodes in multiple sub-assemblies are evident, particularly in the exterior ones. In the remaining sub-assemblies, columns represent the weakest link, either with a flexural or shear mechanism. These mechanisms are indicative of structures designed for gravity loads only, where the design does not consider the hierarchy between elements. Given such hierarchy configuration in the sub-assemblies, the probable collapse mechanism which occurs is the "soft-story" column-sway type. Notably, the

adopted version of the SLaMA method is based on NZSEE regulations, thus employing capacity models and drift limits of structural elements different from the Italian building code (NTC18). This may result in an overestimation of the structural deformation capacity and, consequently affecting the Expected Annual Loss (EAL) calculation.
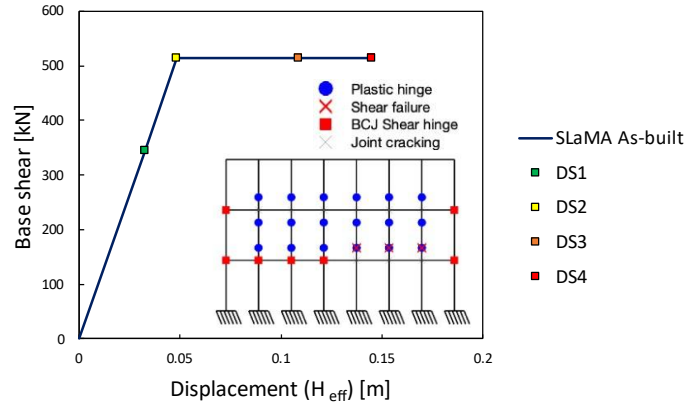

Figure 3. GLD-3-500: SLaMA pushover curves with DS thresholds definition and the prediction of the probable hierarchy

3.3 Template retrofit configurations and fragility-oriented retrofit design

The seismic performance at the LS limit state, defined by the displacement at which the 75% of the ultimate deformation capacity is reached by the first structural element, can be derived by applying the Capacity Spectrum Method (CSM) once the pushover curve has been converted into a single-degree-of-freedom system and plotted on an acceleration-displacement response spectrum format (ADRS). To apply the fragility-oriented approach, three points in the capacity to life-safety demand ratio (CDR_{LS}) versus μ_{DSi} space are needed, where μ_{DSi} is the median of the fragility function at a selected DS. The first point represents the as-built structure, the other two points represent retrofit solutions with higher CDR_{LS} values, but are not necessarily aligned with specific performance objectives. The relationship to be used can be obtained by defining an interpolating line between the considered points for each DS (Figure 4).
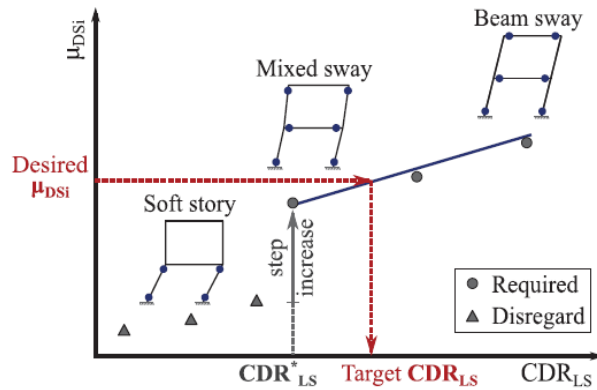

Figure 4. CDR_{LS} vs μ_{DSi} linear fit (Aljawhari et al., Gentile and Galasso, 2022).
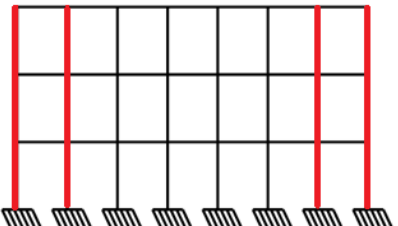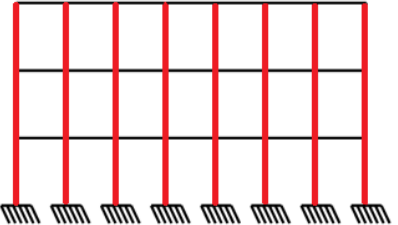
According to the design methodology by Aljawhari et al. (2022), the number of retrofit templates to be considered for a building class depends on the plastic mechanism of the as-built configuration. If the collapse mechanism is mixed, a single retrofit template that transforms the structure into a ductile global plastic beam-sway mechanism (*full retrofit*) can be considered. However, if the original structure exhibits a soft-storey (column-sway) mechanism, at least two retrofit templates are needed: one leading to a mixed mechanism (*partial retrofit*) and the second one resulting in a ductile global collapse beam-sway mechanism (*full retrofit*). Table 1 shows an example of partial and full retrofit for the GLD-3-500 building class.

The implementation cost of each retrofit solution is calculated considering the demolition of the structural/non-structural components to access the jacketed columns, the installation of the intervention itself, and the demolished parts' reconstruction. This evaluation also considers costs related to health/safety and the setting

of the construction site. The foundation improvement cost is considered to be 20% of the jacketing cost and is added only in the cost for the full retrofit intervention. For each building class, only the partial and the full retrofit interventions costs are calculated as described, any intermediate retrofit interventions costs are linearly interpolated.

Figure 5 shows the SLaMA capacity curve for the four building classes in all the considered configurations: as-built, partial and full retrofit. SLaMA results reveal enhanced strength, stiffness, and displacement capacity in building classes with retrofit templates compared to as-built configurations. Notably, the full retrofit template has a more pronounced impact on the displacement capacity of 3-storey building classes, particularly in GLD-3-1000, compared to other classes.

Table 1. – Example of partial and full retrofit intervention for the building class GLD-3-500.

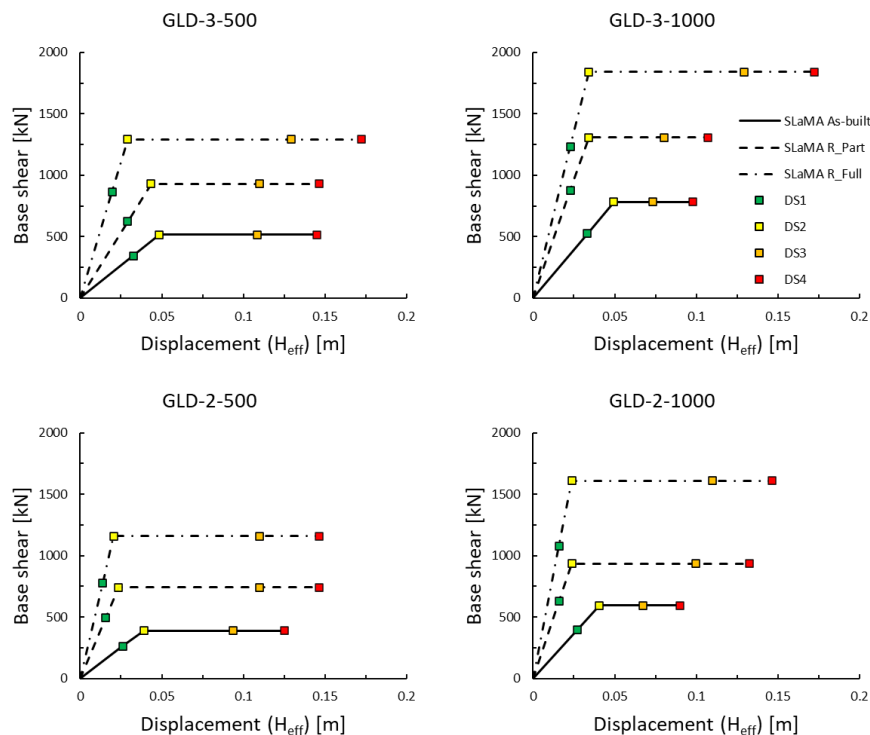| Template	Retrofit description	Graphical illustration
Partial retrofit	Retrofit of the external columns (1st to 3rd storey) with 100 mm jacket reinforced with 10Φ14 mm bars and 1Φ8/150 mm hoops.	
Full retrofit	Retrofit of the external and internal columns (1st to 3rd storey) with 100 mm jacket reinforced with 10Φ16 mm bars and 1Φ8/150 mm hoops.	

Figure 5. SLaMA pushover curves for the four considered building classes for as-built, partial retrofit (R_Part) and full retrofit (R_Full) configurations.

3.4 Fragility assessment

Fragility relationships describe the conditional probability of exceeding different DSs given a ground-shaking intensity measure (IM). Fragility relationships can be established by conducting running the CSM using a set of unscaled ground-motion records (i.e., as-recorded data). This involves creating clouds in the space EDP vs. IM and fitting probabilistic seismic demand models (PSDMs) using a linear regression in the logarithmic space (Eq.1, where *a* and *b* are regression parameters) (Jalayer (2003), Jalayer and Cornell (2009)). Based on the above, lognormal fragility relationships are derived using Eq. 2 (where μ_i and β_i are the median and the logarithmic standard deviation for the ith damage state, respectively). In this study, 150 ground motions selected from the SIMBAD (Selected Input Motion for displacement-Based Assessment and Design) database are adopted consistently with the selection by (Gentile and Galasso (2021b)).

The IM adopted in this study is the 5%-damped spectral acceleration at the first vibration period, i.e., IM=Sa(T_1), while the EDP is assumed as the displacement at effective height (H_{eff}). Figure 6a shows the IM vs EDP cloud and the linear regression for the GLD-3-1000 building class, while Figure 6b and 6c display the fragility curves for different DSs in the as-built configuration and in the two retrofit template configurations. According to Jalayer (2003), the regression analysis is conducted only for non-collapse cases, where collapse cases are here characterized by the attainment of a displacement threshold corresponding to the global instability of the structure. In Figures 7 fragility curves for different DSs in the as-built configuration are plotted for the other three building classes, i.e. GLD-3-500, GLD-2-500, GLD-2-1000. The analyses reveal higher fragility in 3-storey building classes (GLD-3) compared to corresponding 2-storey classes (GLD-2). Additionally, fragility appears to increase across all damage states with the floor area of the building classes.

$$EDP = aIM^b \tag{1}$$

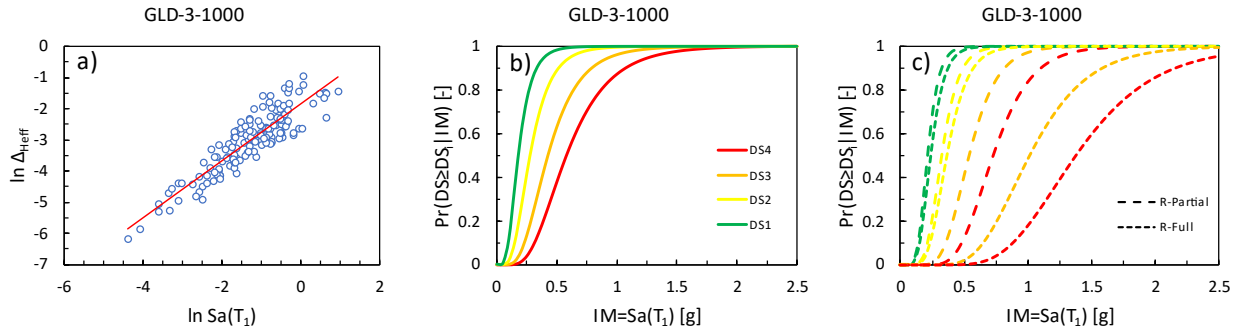$$P(DS \geq DS_i | IM) = \phi\left(\frac{\ln(IM/\mu_i)}{\beta_i}\right) \tag{2}$$

Figure 6. GLD-3-1000 building class: a) IM vs EDP Cloud data with linear regression; b) fragility curves for the as-built configuration for four DS; c) fragility curves for the retrofitted configurations for four DS.
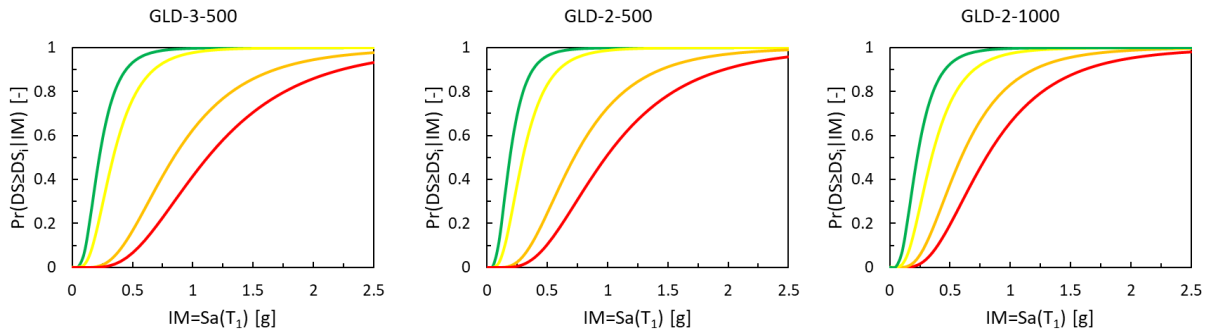

Figure 7. Fragility curves for building classes GLD-3-500, GLD-2-500, GLD-2-1000 in the as-built configuration for four DS.

3.5 Effect of different retrofit solutions on fragility reduction

For each building (8 for each class), the CDR$_{LS}$ values in the as-built and retrofitted (both partial and full) configurations are calculated. The code-base spectra appropriate for each building location are considered. The median values of the fragility functions for the damage state DS3, μ_{DS3}, are plotted versus the CDR$_{LS}$ in Figure 8 for the four classes. Most of buildings in the as-built configurations exhibit a CDR$_{LS}$ <1.

Once relationships are established for each building, it is possible to estimate the reduction in fragility resulting from an increase in the CDR$_{LS}$ value. In particular, in addition to the two retrofit configurations (partial and full) corresponding to the CDR$_{LS}$ values plotted in Figure 8, for the Building #12 (building class GLD-3-1000) assumed as example, in Figure 9a, further five potential performance-target retrofits (corresponding to CDR$_{LS}$ = 0.7, 0.8, 0.9, 1, and 1.1) are reported. For each of these additional CDR$_{LS}$ values, the corresponding median value of the fragility curve at DS3 can be obtained. This comprehensive analysis highlights how the increase in CDR$_{LS}$ by means of several retrofitting solutions may impact the fragility of the structure at DS3 (see the orange curve in Fig. 9b for the Building #12).
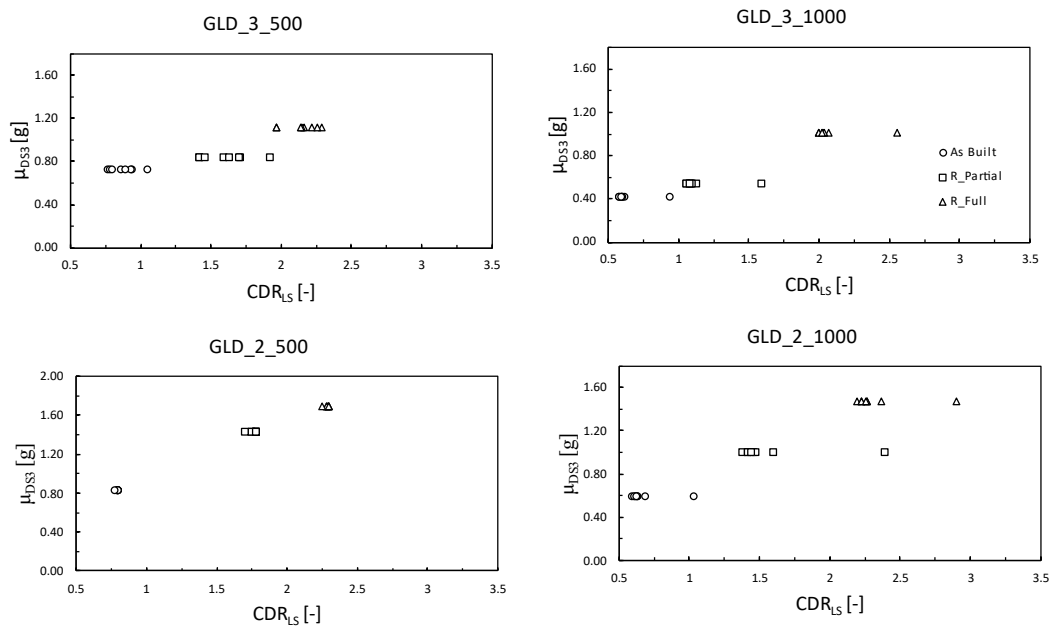

Figure 8. Median value of fragility curves at DS3 vs. CDR$_{LS}$ for all buildings in the portfolio (8 for each class) in the as built and retrofitted configurations (partial and full).

Similar relationships can be derived for the other DSs too, considering for all the DSs the same CDR values assumed for the Life Safety (LS) limit state, i.e. CDR$_{LS}$, that, thus, are performance target values (see Fig. 9a). The interpolation of the median value at each DSs provides an estimate of the fragility parameter for all the considered potential retrofits. Figure 9b shows the fragility curves for Building #12 developed for four DS as CDR$_{LS}$ increases, i.e. for different retrofits. A major reduction in fragility is observed for DS3 and DS4 in comparison with other DSs as CDR$_{LS}$ increases.
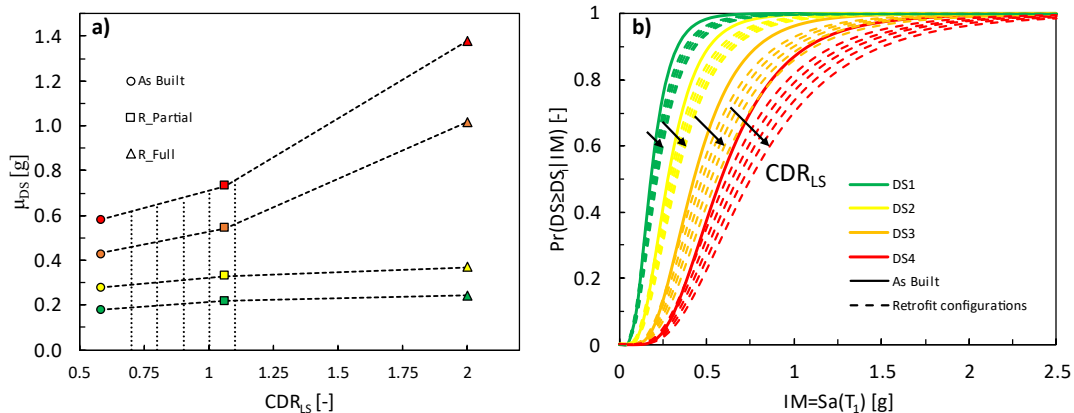
Figure 9. Building #12 (GLD-3-1000 building class): a) median value of fragility curve vs. CDR$_{LS}$ for four DSs; b) fragility curves for the as built configuration and for different retrofitting solutions for four DSs.

3.6 Vulnerability assessment

Vulnerability curves are estimated by employing a consequence model, which connects the repair-to-reconstruction costs to both structural and non-structural DSs. To establish this model, it is essential to determine the expected building-level damage-to-loss ratios (DLRs) for each DS. Using the fragility curves derived for the as built and the retrofitted configurations (both the ones corresponding to the calculated values of CDR$_{LS}$ and the ones obtained by the estimated values of μ_{DS} corresponding to CDR$_{LS}$ = 0.7, 0.8, 0.9, 1, and 1.1), the vulnerability relationships can be obtained for all building classes by means of Eq. 3.

$$\text{LR(IM)} = \sum_{i=1}^{4} \left(F_{DS_{i-1}} - F_{DS_i} \right) DLR \qquad (3)$$

In Eq. 3, F$_{DSi}$ are the ordinates of the fragility curves for a given intensity measure, while DLRs are 0.1, 0.5, 0.75, and 1 for DS1, DS2, DS3, and DS4, respectively. Figure 10a illustrates the vulnerability curves for the building classes in as-built configuration, confirming that the most vulnerable are those with a larger floor area. Furthermore, within the building classes with the same floor area, vulnerability increases with the number of floors. Finally, Figure 10b reports the vulnerability curves for the retrofitted configurations corresponding to CDR$_{LS}$ =1 and shows that for the same retrofit target, there is a variable impact on the building classes. Notably, the vulnerability reduction is more pronounced for the GLD-2-1000 and GLD-3-1000 typologies.
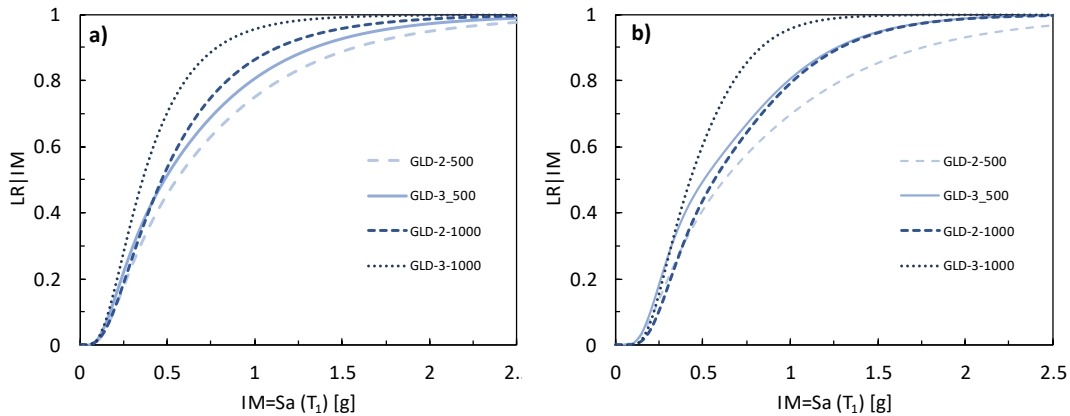

Figure 10. Vulnerability curves for the four considered building classes: a) as built configuration, b) retrofitted configuration corresponding to CDR$_{LS}$=1.

The loss metrics adopted in the study is the EAL, which can be estimated for each building (in as-built and retrofit configurations), adopting a site-specific hazard curve, according to Eq.4, where λ_{IM} is the mean annual frequency of exceeding a given IM, assuming a Poisson distribution.

$$\text{EAL} = \int_0^\infty \text{LR(IM)} \left| \frac{d\lambda_{IM}}{dIM} \right| dIM \qquad (4)$$

Figure 11 displays the 32 site-specific hazard curves utilized for estimating EAL.
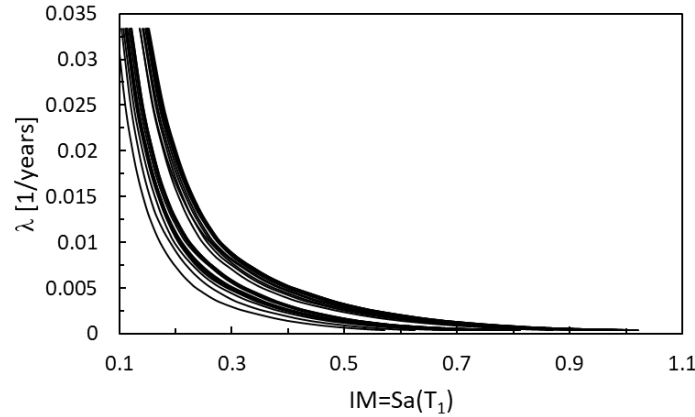
Figure 11. Set of 32 site-specific hazard curves utilized for the EAL estimation.

3.7 Budget allocation

A decision-making process for the optimal allocation of resources consists of finding the solution that minimizes (or maximizes) a desired quantity while taking into account some given constraints. This study builds upon an approach previously developed by Caterino et al. (2018), including the total EAL calculation of the portfolio as a loss metric and assuming a different approach for the fragility estimation of the retrofitted cases. Moreover, the optimal budget allocation solution is detected by using the MILP method.

For each building of the portfolio, the seismic performance in their as-built configuration is defined. The latter is expressed by the CDR_{LS} in the as-built configuration. Starting from this value, a set of increasing CDR_{LS} representative of the improved structures can be achieved.
Buildings with a CDR_{LS} greater than 0.7 are herein considered safe, and no interventions are scheduled for them. The remaining buildings can be improved by increasing the value of CDR_{LS} and estimating the parameters of the fragility curve along the derived relationship. The CDR_{LS} targets defined for potential retrofits are: 0.7, 0.8, 0.9, 1.0, 1.1 (Table 2).As example, if a building has a CDR_{LS} as-built value of 0.4, then potential retrofits may include those that bring the CDR_{LS} to 0.7, 0.8, 0.9, 1, and 1.1.
The total retrofit cost of the portfolio (C_{tot}) is obtained by summing up all the building retrofit costs. Analogously, the EAL of the retrofitted portfolio (EAL_{tot}) is obtained by summing up all the EAL of each building in the assumed retrofit condition.

Table 2. Decision alternatives according to CDR_{LS} values

CDR_{LS}	Decision alternatives
≤ 0.7	(1) Intervention with multiple retrofit templates: CDR_{LS} (potential retrofits) = 0.7, 0.8, 0.9, 1.0, 1.1
> 0.7	(2) No intervention

A MATLAB-based tool is provided to resolve the optimization problem by using a MIPL algorithm which is an optimization linear programming approach where some or all decision variables are integers. The goal of linear programming is to optimize the values of decision variables to maximize or minimize a linear objective function, subject to linear constraints imposed on the decision variables. In this study, the objective function is the EAL_{tot} while the constraint is expressed by the inequality $C_{tot} \leq Budget$ and the decision variables are integers within the range [0-1]. Eq.5 summarises both the objective function and the constraint function of the problem to be solved.

$$\text{Min}(EAL_{tot}) \text{ subjected } to \ \ C_{tot} \leq Budget \qquad (5)$$

As an example, the optimization results are presented for a €2,000,000 budget. Figure 12a illustrates the optimal CDR_{LS} configurations for the adopted retrofit strategy, while Figure 12b provides a breakdown of budget distribution within the portfolio. The results reveal a prioritization of interventions for buildings in classes with larger floor areas. This strategic allocation is driven by the heightened vulnerability of these buildings, given their greater weight in terms of vulnerability within a comparable hazard context. The results underscore

the methodology's ability to strategically allocate resources, maximizing the impact on seismic risk reduction within budget constraints.

The total Expected Annual Loss (EAL$_{tot}$) estimated in the as-built condition is 454,500€. Assuming the optimal retrofitting strategy, the total EAL$_{tot}$ is reduced to 393,700€. A reduction of only 14% in the EAL$_{tot}$ can be observed due to the retrofitting: such a low reduction is related to the averagely high values of the CDR$_{LS}$ evidenced by the buildings of the examined portfolio (i.e., only 14 buildings have CDR$_{LS}$ < 0.7 and, however, the lowest value is 0.55). It is worth noting that the simplified approach herein used to assess the push-over curve (i.e. SLaMA according to NZSEE regulations) may be not sufficiently safe for the typical Italian buildings designed for only gravity loads and this led to have high CDR$_{LS}$ values.

Future developments should adopt a SLaMA-based approach aligned with Italian building code (NTC18) prescriptions. Surely other simplified methodologies should be adopted in the framework of the proposed procedure in order to evaluate the influence of the modelling strategies on the budget allocation and, thus, the results herein presented have to be simply considered as exemplificative of the potentialities of the procedure.
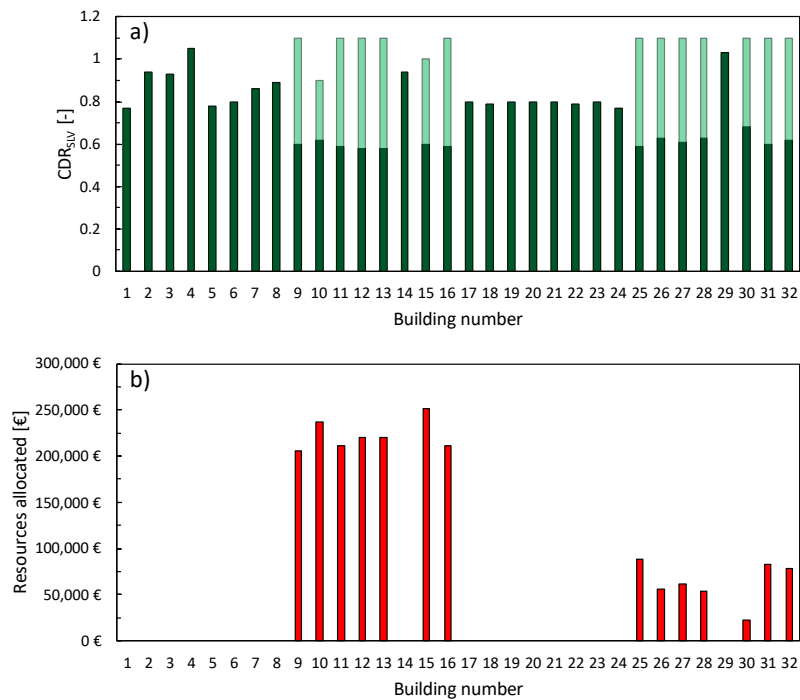

Figure 12. Results of optimization process: a) increase of CDR$_{LS}$ due to portfolio retrofit strategy; b) Budget allocation distribution.

4   Conclusions

This study presents a comprehensive methodology for optimizing seismic risk reduction in large building portfolios with constrained budgets. The methodology integrates building class identification, structural analysis using Simple Lateral Mechanism Analysis (SLaMA), retrofit template configurations, and optimization algorithms. SLaMA identifies probable collapse mechanisms, guiding the formulation of retrofit templates tailored for resilience enhancement.

The fragility analysis is conducted with cloud-analysis method for both as built and retrofitted templates. Mapping the increase in the displacement-based global ratio of capacity to life-safety demand (CDR$_{LS}$) to building-level seismic fragility allows the use of intermediate retrofit solutions (without specific response analyses) and enhances precision in risk assessments.

Expected Annual Loss (EAL) calculations, considering site-specific hazard curves, offer a holistic understanding of portfolio seismic risk under different retrofit scenarios.

Finally, the Mixed Integer Linear Programming (MILP) algorithm optimizes retrofit combinations, minimizing total Expected Annual Loss (EAL$_{tot}$) within budget constraints. The proposed methodology provides a

sophisticated yet practical framework for prioritizing seismic risk mitigation efforts within constrained budgets, contributing to the resilience of built environments in seismic-prone regions.

The results evidenced that the budget allocation is strongly dependent on the modelling strategy adopted for the examined buildings since averagely high values of CDR_{LS} were detected by using the SLaMA approach that led to a low EAL_{tot} reduction after the retrofitting (only 14%). This evidences that the impact of employing different simplified pushover analysis methods has to be deeply investigated in the future, also by comparing results about resource allocation obtained with more accurate numerical analyses.

5   References

Aljawhari, K., Gentile, R. and Galasso, C. (2022) 'A fragility-oriented approach for seismic retrofit design', Earthquake Spectra, 38(3), pp. 1813–1843, https://doi.org/10.1177/87552930221078324.

Borzi, B., Pinho, R. and Crowley, H. (2008) 'Simplified pushover-based vulnerability analysis for large-scale assessment of RC buildings', Engineering Structures, 30(3), pp. 804–820, https://doi.org/10.1016/j.engstruct.2007.05.021.

Calvi, G.M. (1999) 'A displacement-based approach for vulnerability evaluation of classes of buildings', Journal of Earthquake Engineering, 3(3), pp. 411–438, https://doi.org/10.1080/13632469909350353.

Caterino, N., Azmoodeh, B.M. and Manfredi, G. (2018) 'Seismic Risk Mitigation for a Portfolio of Reinforced Concrete Frame Buildings through Optimal Allocation of a Limited Budget', Advances in Civil Engineering, 2018, https://doi.org/10.1155/2018/8184756.

'Freeman 1998_Development and use of capacity spectrum method' (no date).

Del Gaudio, C. et al. (2015) 'Development and urban-scale application of a simplified method for seismic fragility assessment of RC buildings', Engineering Structures, 91, pp. 40–57, https://doi.org/10.1016/j.engstruct.2015.01.031.

Gentile, R. et al. (2019) 'Non-linear analysis of RC masonry-infilled frames using the SLaMA method: part 2—parametric analysis and validation of the procedure', Bulletin of Earthquake Engineering, 17(6), pp. 3305–3326, https://doi.org/10.1007/s10518-019-00584-6.

Gentile, R. et al. (2021) 'Refinement and Validation of the Simple Lateral Mechanism Analysis (SLaMA) Procedure for RC Frames', Journal of Earthquake Engineering, 25(7), pp. 1227–1255, https://doi.org/10.1080/13632469.2018.1560377.

Gentile, R. and Galasso, C. (2021a) 'Simplicity versus accuracy trade-off in estimating seismic fragility of existing reinforced concrete buildings', Soil Dynamics and Earthquake Engineering, 144, https://doi.org/10.1016/j.soildyn.2021.106678.

Gentile, R. and Galasso, C. (2021b) 'Simplified seismic loss assessment for optimal structural retrofit of RC buildings', Earthquake Spectra, 37(1), pp. 346–365, https://doi.org/10.1177/8755293020952441.

Jalayer, F. (2003) Direct Probabilistic Seismic Analysis: Implementing Non-linear Dynamic Assessments Ph.D. Dissertation, Stanford University, California, 2003.

Jalayer, F. and Cornell, C.A. (2009) 'Alternative non-linear demand estimation methods for probability-based seismic assessments', Earthquake Engineering and Structural Dynamics, 38(8), pp. 951–972, https://doi.org/10.1002/eqe.876.

Masi, A. et al. (2019) 'Seismic response of RC buildings during the Mw 6.0 August 24, 2016 Central Italy earthquake: the Amatrice case study', Bulletin of Earthquake Engineering, 17(10), pp. 5631–5654, https://doi.org/10.1007/s10518-017-0277-5.

New Zealand Society for Earthquake Engineering (NZSEE) (2017) The Seismic Assessment of Existing Buildings – Section C2: Assessment Procedures and Analysis Techniques, www.building.govt.nz.

Nettis A, Gentile R, Raffaele D, et al. Cloud Capacity Spectrum Method: accounting for record-to-record variability in fragility analysis using nonlinear static procedures. Soil Dynamics and Earthquake Engineering 150: 106829.

Westerberg, C.-H., Bjorklund, B. and Hultman, E. (1977) An Application of Mixed Integer Programming in a Swedish Steel Mill.